A Journal of the Gesellschaft Deutscher Chemiker

Angewandte International Edition GDCh Chemie

www.angewandte.org

Accepted Article

Title: In-situ Generation of An N-Heterocyclic Carbene-Functionalized Metal-Organic Framework via Postsynthetic Ligand Exchange for Efficient and Selective Hydrosilylation of CO2

Authors: Xu Zhang, Jiao Sun, Guangfeng Wei, Zhipan Liu, Huimin Yang, Kaimin Wang, and Honghan Fei

To be cited as: *Angew. Chem. Int. Ed.* 10.1002/anie.201813064
Angew. Chem. 10.1002/ange.201813064

Link to VoR: http://dx.doi.org/10.1002/anie.201813064
http://dx.doi.org/10.1002/ange.201813064

WILEY-VCH

10.1002/anie.201813064

WILEY-VCH

In-situ Generation of An *N*-Heterocyclic Carbene-Functionalized Metal-Organic Framework *via* Postsynthetic Ligand Exchange for Efficient and Selective Hydrosilylation of CO_2

Xu Zhang,[a] Jiao Sun,[a] Guangfeng Wei,*[a] Zhipan Liu,[b] Huimin Yang,[a] Kaimin Wang,[a] and Honghan Fei*[a]

Abstract: *We report a metal-organic framework (MOF) catalyst that realizes CO_2 to methanol transformation under ambient conditions. The MOF is one rare example containing metal-free N-heterocyclic carbene (NHC) moieties, which are installed using an in-situ generation strategy involving the incorporation of an imidazolium bromide-based linker into the MOF by postsynthetic ligand exchange. Importantly, the resultant NHC-functionalized MOF is the first catalyst capable of performing quantitative hydrogen-transfer from silanes to CO_2, thus achieving quantitative (>99%) methanol yield. Density functional theory calculations indicate the high catalytic activity of the NHC sites in MOFs are attributed to the decreased reaction barrier of a reaction route involving the formation of an NHC-silane adduct. In addition, the MOF-immobilized NHC catalyst shows enhanced stability for up to eight cycles without base activation as well as high selectivity towards the desired silyl methoxide product.*

The chemical transformation of CO_2, a non-toxic, abundant and environmentally friendly C1 source, into fuels such as methanol is of enormous atom-economic and environmental importance.[1] However, this process is energy-intensive, owing to the thermodynamically inert nature of CO_2. A variety of homogeneous catalytic systems are used to transform CO_2 into methanol, including those based on organometallic catalysts,[2] organocatalysts,[3] frustrated Lewis pairs,[4] perrhenate anions[5] and alkali metal carbonates[6]. These systems typically employ hydrosilanes as an environmentally benign reductant. However, they generally achieve only partial reduction to formoxysilanes as the major products, with the desired methoxide products (which can be readily hydrolyzed to methanol) being produced in low yields (<10%).

Nucleophilic N-heterocyclic carbenes (NHCs) can react with CO_2 at the lone pair of carbene electrons to form imidazolium carboxylates.[7] Ying and co-workers reported the first example of NHC-catalyzed reduction of CO_2 with silanes to form methoxide products along with siloxane $(Ph_2(MeO)SiO\text{-})_n$ via formoxysilane intermediates.[8] This catalytic system exhibited high CO_2 reduction efficiency that is superior to other homogeneous systems.[2-6] However, their recent attempts to immobilize the NHC moieties onto polymeric materials significantly lowered the yields of silyl methoxide, and the deactivation of the catalyst was observed after three cycles.[9]

Over the past decade, metal-organic frameworks (MOFs) have garnered increasing research attentions in heterogeneous catalysis owing to their tunable porosities, tailorable functionality and excellent reusability.[10] Accordingly, the high degree of control over the structural and chemical features makes MOFs extremely promising as next-generation CO_2 capture materials,[11] and their ability to promote catalytic conversion of CO_2 to high-value chemicals has been demonstrated.[12] However, the vast majority of MOF-based catalysts for chemical fixation of CO_2 rely on the cycloaddition of CO_2 with three-membered rings or alkyne-containing molecules, which are high-energy starting materials.[12,13] Up-to-date, only two MOF-based catalysts have been reported to successfully realize chemical reduction of CO_2 to methanol[14] or other related intermediates (HCO_2H),[15] but both require harsh conditions including elevated operating temperature (up to 250 °C) and high CO_2 pressure (4-15 MPa). In addition, these catalysts employed MOFs merely as a matrix to confine the catalytically active species in their porosity.[14,15]

The development of NHC-functionalized MOF materials has attracted considerable interests, which are promising to enable size/shape selectivity and recyclability.[16] However, despite many attempts to produce free NHC moieties in aryl- or

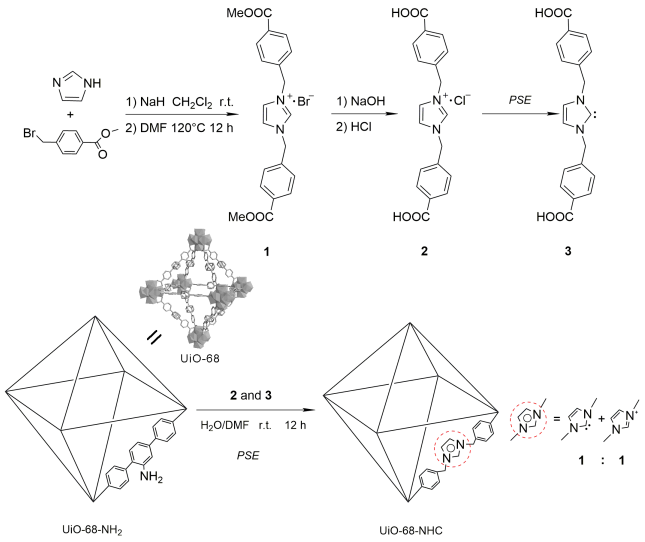

Scheme 1. Schematic representation of UiO-68-NHC synthesis.

[a] X. Zhang, J. Sun, Dr. G. Wei, H. Yang, K. Wang, Prof. H. Fei
Shanghai Key Laboratory of Chemical Assessment and Sustainability, School of Chemical Science and Engineering
Tongji University
1239 Siping Rd., Shanghai 200092, China
E-mail: fei@tongji.edu.cn (H. Fei), weigf@tongji.edu.cn (G. Wei)
[b] Prof. Z. Liu
Collaborative Innovation Center of Chemistry for Energy Material, Shanghai Key Laboratory of Molecular Catalysis and Innovative Materials, Key Laboratory of Computational Physical Science (Ministry of Education), Department of Chemistry
Fudan University, Shanghai 200043, China

Supporting information for this article is given via a link at the end of the document.

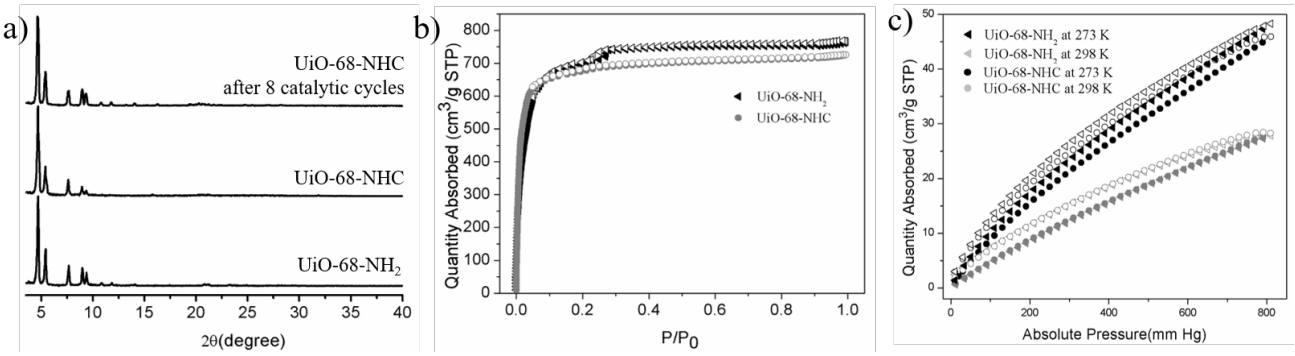

Figure 1. a) PXRD of UiO-68-NH_2, UiO-68-NHC before and after 8 catalytic cycles, b) N_2 isotherms of UiO-68-NH_2 and UiO-68-NHC at 77 K. c) CO_2 sorption of UiO-68-NH_2 and UiO-68-NHC at 273 K and 298 K.

alkylimidazolium-based MOFs, this has not been possible, largely owing to degradation of the MOFs under the strongly basic condition required for deprotonation.[17] To the best of our knowledge, the only example of free NHC-like moieties residing in MOFs was reported by Hupp, Farha and co-workers, who treated a Co^{II}-imidazolate framework with *n*-butyl lithium to generate NHC sites.[18] However, in this material the catalysis occurred exclusively on MOF surfaces, presumably owing to a decrease in crystallinity.

Herein, we report for the first time the incorporation of a free NHC complex into a robust Zr^{IV}-based MOF using postsynthetic ligand exchange (PSE). More importantly, the resultant MOF catalyst is capable of quantitatively transforming silanes to methoxides using CO_2 under extremely mild condition (1 atm and room temperature), and the methoxide product can be completely converted to methanol via hydrolysis.

The imidazolium-based ligand precursor 1,3-bis(4-carboxybenzyl)-1H-imidazol-3-ium bromide (**2**, Scheme 1) was synthesized in high yields in two steps: nucleophilic substitution of imidazole with 4-(bromomethyl)benzoate, followed by hydrolysis. The UiO-68 framework, which comprises $Zr_6O_4(OH)_4$ clusters as metal-oxo nodes and terphenyl-4,4'-dicarboxylate (tpdc) as struts, was chosen as the matrix owing to the similar chain lengths of **2** (~14.5 Å) and tpdc (~15.0 Å). UiO-68-NH_2 was synthesized using a mixture of $ZrCl_4$, 2,5-bis(4-carboxylphenyl)aniline (tpdc-NH_2) and acetic acid (as a modulator) at 70 °C in N,N'-dimethylformamide (DMF) for 72 h. Before PSE, **2** was dissolved in aqueous 4 wt.% KOH solution and DMF to deprotonate the carboxylic acid. After tuning pH to neutral condition with diluted HCl solution, ^{1}H NMR and ^{13}C NMR of the PSE solution confirm the *in-situ* generation (~50% yield) of **3** containing free NHC species *via* the hydrogen abstraction from the imidazolium bromide (Figure S1 and S2). More importantly, ESI-MS(-) of the above mixtures exhibit the characteristic peak of the targeted carbene species (*m/z* 335.1 $[M-H]^-$, Figure S3). In addition, both ^{1}H NMR and ^{13}C NMR demonstrate the mixture of carbene and imidazolium-based ligands are chemically stable in the aqueous condition for over 12 h (Figure S2b and Figure S4).

PSE was performed by incubating the solid UiO-68-NH_2 in the above-mentioned mixture (DMF/H_2O solution containing free carbene species) at room temperature for 12 h. The linker-exchanged material, UiO-68-NHC, was isolated by centrifugation, washed extensively with methanol, and dried under vacuum. Powder X-ray diffraction (PXRD) and scanning electron microscopy (SEM) confirm the retention of the crystalline UiO-68 framework with microcrystals of octahedral morphology (Figure 1a and Figure S5). Digestion of the UiO-68-NHC using diluted HF in d^6-DMSO shows the degree of PSE to be 37% (Figure S6). ^{1}H NMR of the PSE solution shows no obvious change in the molar ratio (1:1) of the NHC-based ligands and the imidazolium-based ligands throughout the substitution process (Figure S1a and S4), evidencing the equimolar ratio of the two incoming ligands into UiO-68. ^{13}C MAS NMR spectroscopy of UiO-68-NHC demonstrates a low-intensity resonance of ~167 ppm (Figure S7), which corresponds well with the carbene/imidazolium carbon shift in the PSE solution (Figure S2). The shift is the average of the carbon resonance in the carbene moieties (~205 ppm) and the imidazolium ligand (~135 ppm), probably owing to the dynamic proton exchange on the NMR time scale.[19]

We continue to confirm the ligand exchange process occurred, as opposed to simple inclusion of **3** inside the MOF pores. First, a control experiment was performed in which UiO-68-NH_2 was treated with a H_2O/DMF solution containing the carboxylic acid ester of the NHC-precursor (**1**, Scheme 1) under the identical conditions as those used for PSE. However, after extensive washing of the resultant MOFs, ^{1}H NMR of the digested MOF solids indicates no inclusion of **1** (Figure S8). This NMR observation indicates the importance of the coordinating carboxylate during PSE. Second, inductively coupled plasma (ICP) and C/H/N elemental analysis (EA) confirm the ligand/Zr ratio did not change throughout the PSE process (see experimental section in ESI). Third, the amount of the tpdc-NH_2 that leached into the solution during PSE process is measured to be ~40%, agreeing with the degree of MOF functionalization (37%) (Figure S4 and S6). Moreover, only a slight decrease of a Brunauer-Emmett-Teller (BET) surface area, measured with N_2 absorption at 77 K, from 2713 m^2/g (before PSE) to 2610 m^2/g (after PSE) is observed (Figure 1b). Indeed, a noticeable hysteresis loop has been observed in UiO-68-NH_2, while UiO-68-NHC only displays a steep rise in the low pressure range without the hysteresis in the desorption branch (Figure 1b). This suggests that the missing-linker defects in the parent UiO-68-NH_2 have been replaced with the incoming NHC-based ligands during PSE process, agreeing with the previous studies.[20] In addition, PXRD and SEM further evidence that the crystallinity of UiO-68-NHC is obviously higher than UiO-68-NH_2

Table 1. Catalytic activity of the hydrosilylation of CO_2 with diphenylsilane, according to ^1H NMR results in Figure 2.[a]

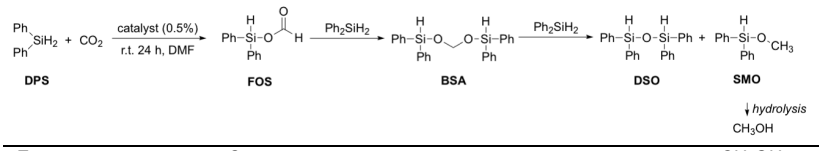

Entry	Catalyst	Conv. (%)[b]	FOS[c]	DSO[c]	BSA[c]	SMO[c]	CH_3OH Yield (%)[d]
1[e]	UiO-68-NHC	0	0	0	0	0	0
2	blank	15	0.002:1	0.039:1	0.017:1	0.024:1	2
3	equimolar KOH-treated **1**	92	0.000:1	0.336:1	0.089:1	0.025:1	2
4	equimolar NaH-treated **1**	>99	0.000:1	0.080:1	0.160:1	0.820:1	81
5	UiO-68-NH_2	32	0.003:1	0.079:1	0.020:1	0.052:1	5
6	UiO-68-NH_2 and PSE-treated **2**	62	0.011:1	0.183:1	0.098:1	0.038:1	4
7	**UiO-68-NHC**	**>99**	**0.000:1**	**0.000:1**	**0.000:1**	**1.000:1**	**>99**
8	**UiO-68-NHC (8th cycle)**	**>99**	**0.018:1**	**0.072:1**	**0.120:1**	**0.900:1**	**90**

[a]Reaction conditions: 1 mmol diphenylsilane, 0.5 mol % catalyst (based on Si-H), 1 mL DMF, 0.1 MPa CO_2, r.t. , 24 h. Mesitylene (1 mmol) was added as an internal standard. [b]The conversion efficiencies were determined using ^1H NMR integration with mesitylene (internal standard). [c]The ratio represents the actual ^1H NMR integration ratio between each characteristic silyl (or silane-based) functional group and the mesitylene (internal standard), according to ^1H NMR in Figure 3 and Figure S12. [d]CH_3OH yield (based on Si-H) is determined using GC-FID with isopropanol as an internal standard. [e]Using 0.1 MPa N_2 instead of CO_2, r.t., 24 h.

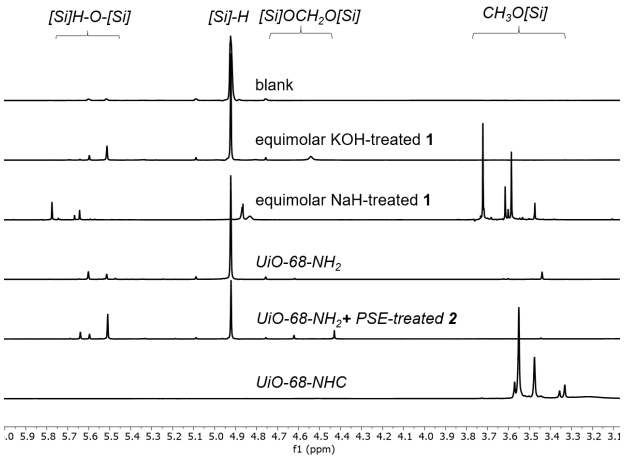

Figure 2. ^1H NMR spectra of hydrosilylation of CO_2 with diphenylsilane using different NHC-based catalysts.

(Figure S10 and S11), consistent with the N_2 adsorption isotherms. Low-pressure CO_2 isotherms reveal the identical CO_2 uptake capacity throughout PSE (Figure 1c), further confirming the ligand metathesis process and not simple encapsulation of **3** within the MOF pores. The increase in the zero-coverage isosteric heat of adsorption (Qst) for CO_2 from 21 kJ mol^{-1} (UiO-68-NH_2) to 26 kJ mol^{-1} (UiO-68-NHC) is most likely due to the interaction between CO_2 and carbene functionalities (Figure S13). Based on these thorough characterization and control experiments, along with high degree of NHC linker incorporation, the results support a ligand metathesis process and against simple trapping of 3 inside the porosity. Indeed, PSE of UiO-type MOFs with several flexible dicarboxylate ligands of similar chain length (*e.g.* UiO-66 vs. adipate) have been reported previously.[21]

Catalytic reduction of CO_2 was first performed using diphenylsilane (DPS) under atmospheric pressure of CO_2 (0.1 MPa) and room temperature. The reduction intermediates and/or products were identified using ^1H NMR. These include formoxylsilane (FOS, δ=8.0~9.0), bis(silyl)-acetal (BSA, δ=4.4~4.8), silyl methoxides (SMO, δ=3.3~3.7), and disiloxane (DSO, δ=5.4~5.8) (Table 1, Figure 2 and S14).[8] $^{13}CO_2$ experiments confirm the initial formation of FOS *via* the MOF catalyst, followed by the direct conversion of FOS to SMO without the detection of the intermediate (BSA) (Figure S15 and S16). Importantly, using UiO-68-NHC with only a 0.5 mol% loading of the carbene sites affords quantitative conversion of DPS to SMO with nearly quantitative selectivity (Table 1, entry 7). Moreover, hydrolysis using two equiv. of NaOH in aqueous solution easily converts SMO to methanol to complete the overall $CO_2 \rightarrow CH_3OH$ (Figure S17-S19), achieving an overall methanol yield of >99% based on Si-H. To the best of our knowledge, this is the first NHC-based catalyst to achieve the ultrahigh selectivity and quantitative methanol yield under ambient condition (1 atm CO_2, r.t.). Moreover, a control experiment to perform the reaction in N_2 instead of CO_2 completely shuts down the silane conversion, verifying that the carbon atoms in final CH_3OH product originate from CO_2 (Table 1, entry 1 and Figure S20).

To directly compare the CO_2 reduction activity of UiO-68-NHC to that of homogeneous catalytic system, we have performed the equimolar KOH treatment towards **1** to attain NHC sites. Despite the catalyst **1** (after equimolar KOH treatment) achieving >90% conversion of diphenylsilane, the major catalytic product is the side product DSO instead of SMO (Table 1, entry 3). Activating the catalyst **1** using equimolar NaH is necessary to give nearly quantitative conversion of silane and >80% silyl methoxide products (Table 1, entry 4), consistent with the previous study (Figure 2).[8] These catalytic studies evidence that the NHC sites in MOFs can be activated under relatively mild condition and avoid using the user-unfriendly strong base (*e.g.* NaH). Meanwhile, using a mixture of UiO-68-NH_2 and carbene sites (PSE-treated **2**) as the catalyst gave 62% conversion of silane with low selectivity towards the final methoxide product (Table 1, entry 6). These control experiment confirm the ordered array of NHC-based struts residing in the framework play an important role in the efficient catalysis.

In order to gain better insights of the catalytic performance of UiO-68-NHC, we have performed density-functional theory (DFT) calculations (see ESI for details) to study the reaction kinetics of the FOS formation step, which has been proved to be the rate-determining step in homogeneous system.[22] There are two possible catalytic reaction routes for the FOS formation, i.e. SAPI (NHC-CO_2 + DPS → FOS) and SAPII (NHC-DPS + CO_2 →

FOS) pathway (Figure S15). The reaction profiles are shown in Figure 3a. Consistent with the earlier study,[22] the calculated reaction barriers (ΔG_a) of SAPII path in homogeneous system ($SAPII_{HOMO}$) is 1.29 eV, slightly lower (0.02 eV) than that of SAPI path ($SAPI_{HOMO}$). However, the ΔG_a of SAPII path in UiO-68-NHC ($SAPII_{MOF}$) is significantly reduced to only 0.96 eV. which is ~0.4 eV lower than the barrier of SAPI path ($SAPII_{MOF}$). The results suggest that the SAPII path is the major reaction route and the high activity of UiO-68-NHC is ascribed to the decrease of ΔG_a of SAPII path.

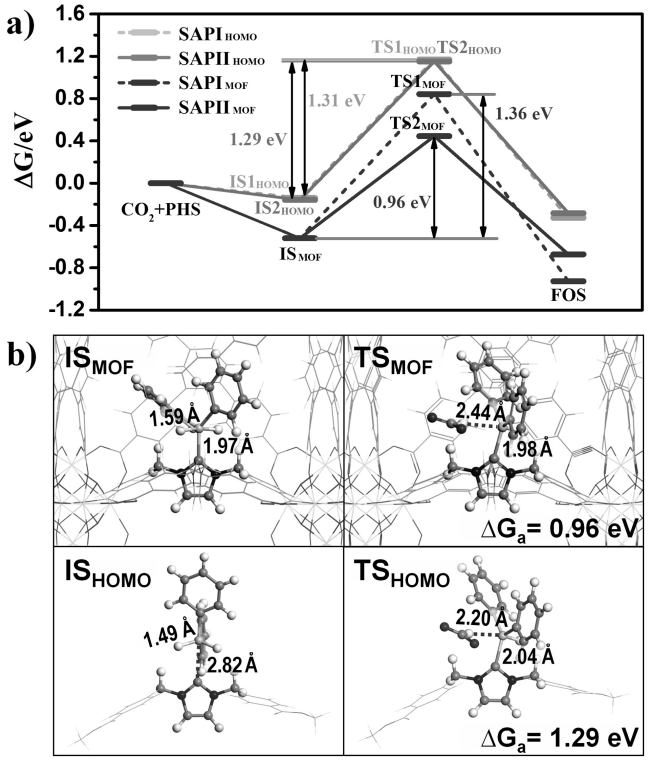

Figure 3. a) The reaction profiles of FOS formation. The ΔG_a of SAPI and SAPII path in homogeneous system is 1.31 and 1.29 eV, respectively. In the MOF system, the ΔG_a of SAPI remains high (1.36 eV), while the ΔG_a of SAPII drops to 0.96 eV. b) The structure snapshots of the ISs and TSs of SAPII path in the channel of MOF (IS_{MOF} and TS_{MOF}) and homogeneous analog (IS_{HOMO} and TS_{HOMO}). Si yellow; O red; N blue; C grey; H white.

We continue to investigate the structures of the initial states (ISs) and transition states (TSs) of SAPII path to evidence the decrease of ΔG_a from UiO-68-NHC. First, MOFs and homogeneous analog show a similar reaction pathway with the initial formation of the silane-NHC adducts, followed by the H atoms from silanes attacking the C atoms of diffused CO_2 molecules to achieve the TS (Figure 3b). The major difference between the UiO-68-NHC and the homogeneous analog is that the Si-H bonds in IS_{MOF} (1.59 and 1.57 Å) are substantially longer than the corresponding bonds in IS_{HOMO} (1.49 Å), which implies that the H atoms of DPS in IS_{MOF} is more readily to dissociate and transfer to the CO_2. This is attributed to the strong host-guest interactions between the DPS molecules and the NHC sites in IS_{MOF}, probably owing to the confined porosity of UiO-68. Moreover, the Si-C distance at IS_{MOF} is only 1.97 Å, which is 0.85 Å closer than that at IS_{HOMO} (Figure 3b). The Si-C distance of TS_{MOF} is 1.98 Å, 0.06 Å shorter than that of TS_{HOMO} as well. These values indicate the incorporation of NHC moieties into MOFs substantially enhances the reactivity towards silane precursors, which is consistent with the fact that the formation of Si-C bond in silane-NHC adduct in MOF is more exothermic than that in homogeneous systems (Figure 3a). .

Meanwhile, in the SAPI mechanism, the formation of NHC-CO_2 adduct at the IS is followed by transfer of H atoms from DPS to CO_2 to achieve the TS. No direct interaction is observed between the DPS and NHC in this pathway, thus the ΔG_a in UiO-68-NHC and homogeneous analog are very close (*i.e.* 1.36 eV for UiO-68-NHC and 1.31 eV for homogeneous analog).

Solvent screening tests reveal a high selectivity toward SMO in basic polar solvents, including DMF, DEF and TEA (Table S2, entry 1-3). However, no reaction is detected in neutral solvents, probably due to that the Lewis basicity of the solvents helps in Si-H bond activation (Figure S21).[15] UiO-68-NHC exhibits excellent recyclability with almost no decrease in yield and selectivity over at least six cycles in DMF, DEF and TEA (Table 1 entry 8, and Table S1). The high crystallinity of the recycled UiO-68-NHC catalyst is confirmed by PXRD and SEM (Figure 1a and S3). Unlike the homogeneous catalyst, the site-isolated NHC moieties residing in our MOF catalyst are active for up to 60 h with a turnover number (TON) of 1700 and a turnover frequency of 28.5 h^{-1} using merely 0.05 mol% of UiO-68-NHC (Table S2 entry 6). Increasing the catalyst loading to 2.5 mol% or the reaction temperature to 60 °C allows for completion of the reaction with a quantitative yield of SMO in only 5 h (Table S2 entry 4 and 5).

In addition, we have employed both control experiments and theoretical calculations to investigate why UiO-68-NHC has a significantly enhanced selectivity towards SMO products. First, we perform absorption experiments between UiO-68 and a mixture of products (SMO and DSO). After incubation for 12 h, digestion of MOF with diluted HF in $CDCl_3$ and ^1H NMR analysis revealed that SMO is the dominating guest molecules residing in the MOF porosity (Figure S22). Moreover, DFT calculations of the diffusion kinetics are employed to show that the diffusion of DPS, SMO and DSO inside the porosity (Figure S23). The barrier for the diffusion of the precursor (DPS) and the desired product (SMO) within MOF are both ~0.69 eV. Meanwhile, the diffusion barrier of DSO significantly increases to 1.42 eV, owing to its larger size. Moreover, it is found that the DPS molecules energitically perfer to attach onto the NHC sites, while the final SMO product tends to adsorb in the porosity of UiO-68-NHC *via* the π-π intercations between SMO and the phenyl rings on the MOF struts. These results confirm that the silane precursors tend to diffuse to the NHC sites in MOFs and the methoxide product prefers to diffuse into the MOF channel after the reaction. However, the side-product molecules are more likely to stay at the NHC sites for further reactions, owing to the high diffusion barrier. This also explains why we do not observe intermediates in our MOF-catalyzed $^{13}CO_2$ experiments. The molecular size calculations further indicate all of the silyl-based intermediates/products comfortably reside in the pore cavities of UiO-68-NHC, but only the diffusion of SMO through the pore windows of UiO-68 is easier than that of other products and intermediates (Figure S24).

In conclusion, we have developed the first MOF catalyst realizing the chemical reduction of CO_2 to methanol under ambient conditions. Compared to the homogeneous NHC-based catalyst, the well-defined porosity of UiO-68-NHC achieves

superior activity and selectivity towards the desired silyl methoxide product. This work reveals the enormous potential for functionalized MOFs as nanoscale reactors that selectively convert CO_2 to target value-added chemicals.

Acknowledgements

This work was supported by grants from the National Natural Science Foundation of China (51772217, 21603165), the Recruitment of Global Youth Experts of China, the Fundamental Research Funds for the Central Universities, Shanghai Sailing Program (16YF1412300) and the Science & Technology Commission of Shanghai Municipality (14DZ226110).

Keywords: metal-organic frameworks • *N*-heterocyclic carbene • CO_2 fixation • heterogeneous catalysis • density functional theory

[1] Sakakura, T.; Choi, J.-C.; Yasuda, H. *Chem. Rev.* **2007**, *107*, 2365–2387. b) Lu, X.-B.; Darensbourg, D. J. *Chem. Soc. Rev.* **2012**, *41*, 1462–1484. c) Trickett, C. A.; Helal, A.; Al-Maythalony, B. A.; Yamani, Z. H.; Cordova, K. E.; Yaghi, O. M. *Nat. Rev. Mater.* **2017**, *2*, 17045.

[2] a) Courtemanche, M.-A.; Larouche, J.; Légaré, M.-A.; Bi, W.; Maron, L.; Fontaine, F.-G., *Organometallics* **2013**, *32*, 6804-6811; b) Stephan, G. M. *J. Am. Chem. Soc.* **2010**, *132*, 1796-1797.

[3] a) Courtemanche, M. A.; Legare, M. A.; Maron, L.; Fontaine, F. G. *J. Am. Chem. Soc.* **2013**, *135*, 9326-9329; b) Declercq, R.; Bouhadir, G.; Bourissou, D.; Légaré, M.-A.; Courtemanche, M.-A.; Nahi, K. S.; Bouchard, N.; Fontaine, F.-G.; Maron, L. *ACS Catal.* **2015**, *5*, 2513-2520.

[4] a) Chen, J.; Falivene, L.; Caporaso, L.; Cavallo, L.; Chen, E. Y. *J. Am. Chem. Soc.* **2016**, *138*, 5321-5333; b) Jiang, Y.; Blacque, O.; Fox, T.; Berke, H. *J. Am. Chem. Soc.* **2013**, *135*, 7751-7760; c) Khandelwal, M.; Wehmschulte, R. J. *Angew. Chem. Int. Ed.* **2012**, *51*, 7323-7326; d) Berkefeld A.; Masood P. *J. Am. Chem. Soc.* **2010**, *132*, 10660-10661.

[5] Morris, D. S.; Weetman, C.; Wennmacher, J. T. C.; Cokoja, M.; Drees, M.; Kühn, F. E.; Love, J. B., *Catal. Sci. Technol.* **2017**, *7*, 2838-2845.

[6] Fang, C.; Lu, C.; Liu, M.; Zhu, Y.; Fu, Y.; Lin, B.-L. *ACS Catal.* **2016**, *6*, 7876-7881.

[7] a) Jacquet, O.; Gomes, C. D., Ephritihkine, M.; Cantat, T. *J. Am. Chem. Soc.* **2012**, *134*, 2934-2937. b) Das, S.; Bobbink, F. D.; Laurenczy, G.; Dyson, P. J. *Angew. Chem. Int. Ed.* **2014**, *53*, 12876-12879.

[8] Riduan, S. N.; Zhang, Y.; Ying, J. Y. *Angew. Chem. Int. Ed.* **2009**, *48*, 3322-3325.

[9] Riduan, S. N.; Ying, J. Y.; Zhang, Y. *J. Catal.* **2016**, *343*, 46-51.

[10] a) Liu, J.; Chen, L.; Cui, H.; Zhang, J.; Zhang, L.; Su, C.-Y. *Chem. Soc. Rev.* **2014**, *43*, 6011–6061; b) Gascon, J.; Corma, A.; Kapteijn, F.; Llabrés i Xamena, F. X. *ACS Catal.* **2014**, *4*, 361–378; c) Gao, C.; Wang, J.; Xu, H.; Xiong, Y. *Chem. Soc. Rev.* **2017**, *46*, 2799–2823; d) Zhu ,L.; Liu, X.-Q.; Jiang, H.-L.; Sun, L.-B. *Chem. Rev.* **2017**, *117*, 8129–8176; e) Xie, X.-Y.; Qian, X.-Y.; Qi, S.-C.; Wu, J.-K.; Liu, X.-Q.; Sun, L.-B. *ACS Sustainable Chem. Eng.* **2018**, *6*, 13217-13225.

[11] Sumida, K.; Rogow, D. L.; Mason, J. A.; McDonald, T. M.; Bloch, E. D.; Herm, Z. R.; Bae, T.-H.; Long, J. R. *Chem. Rev.* **2012**, *112*, 724–781.

[12] a) Gao, W.-Y.; Chen, Y.; Niu, Y.; Williams, K.; Cash, L.; Perez, P. J.; Wojtas, L.; Cai, J.; Chen, Y.-S.; Ma, S. *Angew. Chem. Int. Ed.* **2014**, *53*, 2615–2619. b) Li, P.-Z.; Wang, X.-J.; Liu, J.; Lim, J. S.; Zou, R.; Zhao, Y. *J. Am. Chem. Soc.* **2016**, *138*, 2142–2145; c) Beyzavi, M. H.; Klet, R. C.; Tussupbayev, S.; Borycz, J.; Vermeulen, N. A.; Cramer, C. J.; Stoddart, J. F.; Hupp, J. T.; Farha, O. K. *J. Am. Chem. Soc.* **2014**, *136*, 15861–15864; d) He, H.; Perman, J. A.; Zhu, G.; Ma, S. *Small* **2016**, *12*, 6309–6324.

[13] a) Zhang, G.; Wei, G.; Liu, Z.; Oliver, S. R. J.; Fei, H. *Chem. Mater.*, **2016**, *28,* 6276–6281. b) Liu, X.-H.; Ma, J.-G.; Niu, Z.; Yang, G.-M.; Cheng, P. *Angew. Chem., Int. Ed.*, **2015**, *54,* 988–991; c) Zhang, G.; Yang, H.; Fei, H. *ACS Catal.*, **2018**, *8,* 2519–2525.

[14] An, B.; Zhang, J.; Cheng, K.; Ji, P.; Wang, C.; Lin, W. *J. Am. Chem. Soc.*, **2017**, 139, 3834-3840.

[15] Li, Z.; Rayder, T. M.; Luo, L.; Byers, J. A.; Tsung, C.-K. *J. Am. Chem. Soc.* **2018**, 140, 8082-8085.

[16] a) Chun, J.; Jung, G.; Kim, H. J.; Park, M.; Lah, M. S.; Son, S. U. *Inorg. Chem.* **2009**, *48*, 6353-6355; b) Kong, G.-Q.; Ou, S.; Zou, C.; Wu, C.-D. *J. Am. Chem. Soc.* **2012**, *134*, 19851-19857; c) Burgun, A.; Crees, R. S.; Cole, M. L.; Doonan, C. J.; Sumby, C. J. *Chem. Commun.* **2014**, *50*, 11760-11763; d) Crees, R. S.; Cole, M. L.; Hanton, L. R.; Sumby, C. J. *Inorg. Chem.* **2010**, *49*, 1712-1719.

[17] Oisaki, K.; Li, Q.; Furukawa, H.; Czaja, A. U.; Yaghi, O. M. *J. Am. Chem. Soc.* **2010**, *132*, 9262-9264.

[18] Lalonde, M. B.; Farha, O. K.; Scheidt, K. A.; Hupp, J. T. *ACS Catal.* **2012**, *2*, 1550-1554.

[19] Tapu, D.; Dixon, D. A.; Roe, C. *Chem. Rev.* **2009**, *109*, 3385-3407.

[20] Park, J.; Wang, Z. U.; Sun, L.-B.; Chen, Y.-P.; Zhou, H.-C. *J. Am. Chem. Soc.* **2012**, *134*, 20110-20116.

[21] Hong, D. H; Suh, M. P. *Chem. Eur. J.* **2014**, *20*, 426-434.

[22] Huang, F.; Lu, G.; Zhao, L.; Li, H.; Wang, Z.-X. *J. Am. Chem. Soc.* **2010**, *132*, 12388-12396.

10.1002/anie.201813064

WILEY-VCH

Entry for the Table of Contents

COMMUNICATION

We report a metal-organic framework containing metal-free *N*-heterocyclic carbene moieties that performs quantitative hydrogen-transfer from silanes to CO_2, thus realizing CO_2 to CH_3OH transformation under ambient conditions.

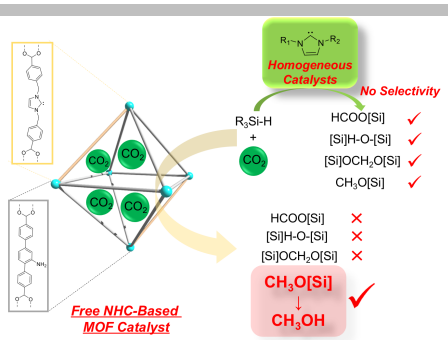

*Xu Zhang, Jiao Sun, Guangfeng Wei, Zhipan Liu, Huimin Yang, Kaimin Wang, Honghan Fei**

Page No. – Page No.

In-situ Generation of an N-Heterocyclic Carbene-Functionalized Metal-Organic Framework *via* Postsynthetic Ligand Exchange for Efficient and Selective Hydrosilylation of CO_2